



Prediction of Flow Resistance Coefficient Correction in Modified Pipe Bends

Moh Abduh^{1,*}, Khairul Iqbal², Sulianto³

¹ Department of Civil Engineering, Faculty of Engineering, Universitas Muhammadiyah Malang, Malang, East Java 65144, Indonesia

² Department of Civil Engineering, Faculty of Engineering, Universitas Syiah Kuala, Banda Aceh, Aceh 23111, Indonesia

³ Department of Civil Engineering, Faculty of Engineering, Universitas Muhammadiyah Malang, Malang, East Java 65144, Indonesia

ARTICLE INFO

Article history:

Received 12 December 2024

Received in revised form 12 January 2025

Accepted 9 February 2025

Available online 31 March 2025

Keywords:

Curvature ratio; modified bend; prediction; correction factor

ABSTRACT

This research is a correction of the empirical equation in previous research. It was aimed at minimising the difference between the final equation and the actual flow. The new parameter that appears is a correction based on validation of the results of the physical model analysis against the initial empirical equation. The final empirical model is influenced by the type of material, flowing flow, bend radius, pipe diameter, number of bend slices (n) and friction coefficient. Model accuracy test include NSE = -0.632 to +0.994, MAE = +0.021 to +1.699 and RMSE = +0.031 to +1.817. The optimum accuracy value achieved on curvature ratio (R/D) 2 up to 4. The best performance is achieved at the minimum resistance coefficient value, on curvature ratio (R/D) = 3 with a single slice and the curvature ratio (R/D) 3.5 with 2 to 5 slices. The result of the correction factor value of the resistance coefficient (ϖ) = $1.3784 n^{0.2077}$ on curvature ratio (R/D) 2, $\varpi = 1.2996 n^{-0.296}$ on curvature ratio (R/D) 3 and $\varpi = 1.4095 n^{-0.357}$ on curvature ratio (R/D) 4. A lower value of the curvature ratio (R/D) and the smaller number of slices on bends (n), the greater vortex at the angle of changes in pipe direction. The vortex is a series of turbulence occurrences at the bend; turbulence symptoms are formed when the flow approaches the bend.

1. Introduction

Flow resistance in pipes is a phenomenon that is often encountered in piping systems [14], whether in household installations, industry or city infrastructure. These caused by various physical aspects of a flowing fluid network [8,15,27], especially related to the pipe material, type of fluid and shape of the pipe bend. This is overcome by appropriate pipe, routine pipe maintenance, using filters to prevent blockages and optimal flow. Also, efficiency of pump and coating materials to reduce flow resistance.

Related research, such as a simple equation for the coefficient of pressure drop in slice bends [4,7], flow behaviour in slice bends [5] and pressure drop coefficient at a 90-degree pipe bend [3] was carried out regarding phenomena flow, simple equation approaches and flow behaviour in 90-

* Corresponding author.

E-mail address: abduh@umm.ac.id (Moh Abduh)

degree bends with slice model. Other studies show the visual similarity of steady and oscillatory flow cross sections and the type of vortex detected in the cross sections. (steady, transient and pulsatile flow [34]) are not identically with the classic Lyne vortex pairs (oscillatory flow) [22]. With an empirical approach and software simulation [11]. This is under the objectives and real conditions in the field.

Developing concepts based on initial research, with hypotheses and simulations. Based on this research, the analysis results are very suitable [3-5] and provide an appropriate description. In physical model, the calibration process is carried out carefully and the results obtained reflect the actual situation. The calibration discharge with triangular and rectangular threshold measuring instruments [1,2,16], also such as in open channel bends [26]. However, the results still need to be developed to provide a more complete result. The basic concepts to refer to in this research are the coefficient of pressure drop (C_{pd}) as follows [3].

$$C_{pd} = \left[f \left(\frac{n L_i}{D} \right) + (1 - \cos^2 \alpha \cos^{(n-1)} 2\alpha) \right] \quad (1)$$

Based on previous research, pressure drop in straight pipes is mainly caused by friction, while in bends it is caused by friction and the impact of the bend [12]. Likewise, in straight pipes using PIV, the results show that the interface morphology determines the direction of the secondary flow pattern [29]. Pressure drop through straight and curved pipes increases with velocity [20]. The velocity vector distribution shows secondary motion caused by fluid movement from the inner wall to the outer wall of the bend, which causes flow separation [13]. Prediction of the selected turbulence model with LDA (Laser Doppler anemometer), the Reynolds influence on the intensity of the secondary vortex flow is a strong function of the bend radius of curvature and a weak function of the Reynolds number [32]. The dissipation of vortex intensity that occurs is exponential [19].

Pressure drop in bends with different turning angles shows an “increase-decrease-increase” trend. The smaller the 90-degree bend radius, the greater the centrifugal force on the flow; the secondary flow phenomenon is more obvious [31]. In a CFD simulation of liquid-solid particle flow in bends, head loss increases with increasing flow velocity [24]. In addition, flow disturbances occur upstream of the bend, downstream velocity is not ideal and velocity fluctuations tend to decrease [33]. Previous research on the characteristics and behaviour of flow in pipe bends tends to be carried out on curved pipe bends [6,9,17,18,25]. Considering these conditions, it is necessary to carry out further studies with a physical model approach.

2. Methodology

2.1 Material and Concept

The modified bend in the form of a slice is an alternative bend that is flexible in terms of curvature, both the radius and angle of the bend. The concept and hypothesis are developed according to empirical studies and should be identical to the actual flow. The concept of mathematical-physical thinking is formed based on models and related materials, The Darcy-Weisbach law in steady laminar flow through a pipe [21]. The model is the idea of the shape of the bend (radius of the bend and number of slices), while the material is related to the pipe used and the type of fluid flowing [3].

Based on the results of analysis of the previous research as in Eq. (1), which includes elements, friction coefficient (f) depends on the roughness of the pipe wall and the type of fluid flowing, the radius of bend (R), the length of the slice axis (L_i), the number of slice modifications (n), the pipe diameter (D), the arc angle of one slice ($\theta = (\text{angle of bend})/n$), angle of direction change ($\alpha = \theta/2$). Using equation (1), then several treatments for different were developed based on this equation with

variations in the number of slice modifications (n) and selecting of flowing fluid, such as water and also the type of pipe. So, by selecting several types of elements, other generation data can be obtained, so that simulations using empirical equations can be run and obtain the desired resistance coefficient and pressure drop values.

With the same conditions as the simulation above, it is then carried out using the Ansys simulation, which aims to monitor pressure changes due to resistance in the modified bends used. Apart from that, this condition also aims to determine the flow behaviour that occurs when passing through the modified bend. By using various models of modification bends, with hope, the flow behaviour that occurs appears to be equal to the hypothesis being developed. With Ansys simulation, you can also know the flow changes that occur while passing through obstacles in all the bend models, including types of flow and the flow changes.

Next, an evaluation of the performance of the modification bend was based on mathematical-physical concepts or empirical equations. Performance evaluation with the flow behaviour approach using Ansys simulation and compared with the results of analysis based on physical models in the laboratory. According to the results of the physical model analysis in the laboratory, differences and similarities can be identified. If the trends that arise from the empirical equations or Ansys simulations show conformity are identical to the physical model in the laboratory, then the empirical equations and Ansys simulations are equal to the actual phenomenon. So, the results obtained are very satisfactory or acceptable, even though empirical correction is still needed so that the trends that emerge coincide with the results of data analysis of physical model generation in the laboratory.

2.2 Geometry

The installation network is connecting between one pipe and another to form a single unit, which functions as a means of delivering fluids from the source to the service point. To unite a network, accessories are needed in the form of bends. To make it easier or more flexible to prepare bend connections, it is necessary to use flexible bends according to the network angle and space conditions. Thus, modifying bend joints using slices is an alternative.

Of course, the concept of a modified bend has a greater obstacle than curved bends but has the advantage of flexibility in terms of bend conditions. The geometry of bends formed in a slice bend modification includes several elements that influence it, including the bend angle, pipe diameter (D) and the number of modified slices (n). The number of modified slices in a bend will result in the length of the slice, which will influence the amount of friction and the magnitude of the angle of change in flow direction (α) as well as the number of changes in flow direction. Referring to the concept, a straight line is a collection of very many and close points, then a curved line is a collection of very many points and forms a tight curve.

The modified slice bends consist of many slices arranged in a curved and tight shape. The modified slice bends with a greater number of slices will have less resistance, resembling the resistance in a curved bend. If slice modification bends are made with a very large number of wedges, it is not simple to assemble, so it is necessary to review the optimal number so that the geometry chosen is optimal in terms of the performance of the bend and its assembly. An example of the geometric model in question is shown in the image below [3].

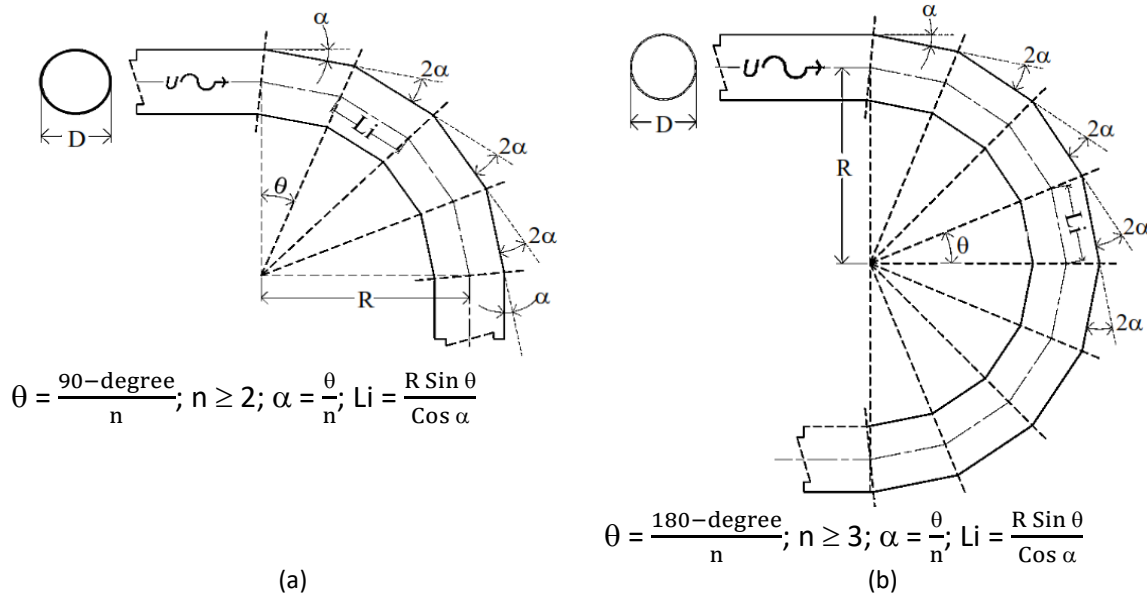


Fig. 1. Geometry model of slice modification bend (a) 90-degree bends with number of slices (n) 4 (b) 180-degree bends with number of slices (n) 8

Based on Figure 1(a). Use the bend angle of 90 degrees with 4 slice modifications that can be arranged with a minimum of 1 slice. What this means is that this modification of the bend allows it to be arranged starting with a minimum number of 1 slice to infinity, as long as it is possible to do so. Meanwhile, Figure 1(b). shows that this bend has the requirement of at least 2 slices in it. This aims to meet these requirements so that the transition angle that is arranged is smaller than 90 degrees so that the fluid can still flow even though the resistance or pressure drop is still high. Thus, the more modifications of slices arranged in a bends, the smaller the resistance, but the more difficult it is to assemble.

2.3 Prediction of Pressure Drop Coefficient

In this research, physical modelling functioned as control and calibration of the model simulation results. Do the simulation results obtained produce trends that are followed under the results of laboratory physics modelling? Likewise, do the flow behaviour and performance demonstrated by the software simulation also depict identical changing conditions? Physical modelling in the laboratory is a depiction of the natural flow that occurs in the fluid flow of pipe networks. Based on this philosophy, all simulation results obtained can be developed according to the results of the physical modelling carried out.

Because this research aims to measure the correction factor of the resistance coefficient in the empirical equation that has been developed, the results of the empirical equation simulation are analysed and developed in such a way that the trends resulting from the empirical equation simulation are corrected mathematically as well as graphically. The results corrections of empirical equation simulation are correction factors generated for the empirical equation of the flow resistance coefficient in the modified bend and can be in the form of a mathematical equation.

The prediction of the resistance coefficient is an empirical equation that has been corrected by a correction factor. The correction factor results from the analysis of the empirical simulation from the equation of the results of physical modelling in the laboratory.

The corrected resistance coefficient is an empirical equation that has been corrected, so the generation value results from the corrected empirical equation. To provide a value result that

coincides with or is identical to the values from the results of physical modelling in the laboratory. Furthermore, the corrected resistance coefficient values along with related elements from the results of this research are used as recommendations based on consideration of optimal coefficient analysis, which provides optimal overall benefit values.

Table 1

Parts of the empirical equation (coefficient of pressure drop) modified bends

No.	Section of obstacle	Values of Parts in Empirical Equations	Notes
1.	Material (δ_a)	$f \left(\frac{n Li}{D} \right)$	Friction (f), number of slices (n), diameter (D), length of slice (Li); Friction factor is influenced by wall roughness and fluid viscosity
2.	Geometry (δ_b)	$(1 - \cos^2 \alpha \cos^{(n-1)} 2\alpha)$	The angle of direction change (α), number of slices (n), radius of bend (R) and each slice angle (θ); The obstacles are affected by sudden direction changes, the more slices there are, the smoother the change in direction and the smaller the obstacle.

Source: Previous research elaboration [3]

3. Results and Discussion

Based on the results of the analysis of empirical equation and physical model tests, they are evaluated for each result and then can be considered. Evaluation of the data distribution trends formed between empirical equation simulations and physical model tests aims to determine the suitability of the trends formed from the data resulting from the analysis. Of course, the trend obtained will not be the same or close to the trend of physical model test data. However, if the trend formed has an identical rhythm, then this condition illustrates the compatibility between the results of the empirical equation and the results of physical model treatment in the laboratory.

The treatments implemented in this research include various conditions of selected curvature ratios. The curvature ratios taken include bend radius (R) = 2D, 3D and 4D. Based on the analysis results obtained between the empirical simulation and the physical model, the trends formed for all curve ratio conditions show identical and uniform results. The trend obtained for all conditions is that the greater the number of slices (n) in a modified bend, the smaller the resulting pressure drop.

At a curvature ratio (R/D) of 2, the occurs of pressure drop value has quite a significant difference, the occurs of pressure drop in physical model simulation is quite high above the numerical simulation results with a coefficient of determination (R²) value in the physical model of 0.9053 and the empirical simulation of 0.983 or a significant level above 90%. Likewise, at a curvature ratio (R/D) of 2, the value of the pressure drop that occurs has a significant difference in magnitude; the occurs of pressure drop in the physical model simulation is quite high above the results of the numerical simulation. The trend that appears from the analysis results shows that the empirical equations used have a pattern that is identical to the physical model.

For a curvature ratio (R/D) of 3, the value of the pressure drop between the physical and empirical models occurs in the slice modification (n) = 2 and in other slice modifications they tend to be close together or identical and the value of the coefficient of determination (R²) in the physical model is 0.8928 and empirical simulation 0.9871 or a significant level above 89%. At a curvature ratio (R/D) of 3, the occurs of pressure drop values have insignificant differences and tend to coincide or be close together. The trend that is built from the analysis results as shown in Figure 2 shows an even similarity. This means that the empirical equations used have a pattern that is identical to the physical model and is quite optimal.

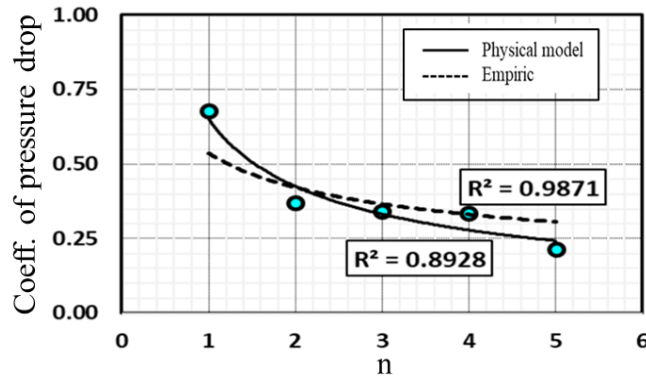


Fig. 2. Pressure drops in modified bends with variations in slices at a curvature ratio (R/D) of 3

Meanwhile, at a curvature ratio (R/D) of 4, the value of pressure drop between the physical and empirical models occurs when the slice modification (n) < 2 and other slice modifications also tend to be close or identical but not the same, at the curvature ratio (R/D) 3 and the coefficient of determination (R^2) in the physical model is 0.4693 and empirical simulation is 0.9908 or a lower significant level. The pressure drops that occur have differences that tend to be close together. The trend that appears from the analysis results with the curvature ratio (R/D) = 4 also shows the empirical equations are identical to the physical model.

Based on the results of the physical model analysis and empirical simulation above, the pressure drop that occurs can then be developed as a correction factor for the pressure drop coefficient at the bend. Furthermore, with this condition, it is necessary to analyse the influence of the related model parameters using the coefficient of determination (R^2). Using regression analysis aims to determine the most appropriate model for predicting the magnitude of the observed data parameters, namely the curvature ratio of turns and the parameter number of slices in turns which have a strong influence on model formation.

The best performance of the parameters resulting from regression analysis and variance analysis was used to develop the number of modified curved slices. These considerations are given with the intention that the results obtained in developing this model have optimal and efficient performance. With this aim, correction factors need to be included in the empirical equation so that it is identical to the physical model conditions. Further testing relates to the accuracy of the empirically developed model to predict values using Nash-Surtcliffe Efficiency (NSE), mean absolute error (MAE) and root mean square error (RMSE) analysis.

To obtain the correction factor for the empirical model and by following the physical model data, the following steps include carrying out a linear regression test to find the correction factor for the pressure drop coefficient between the empirical data and the physical model data for each modified bend model (n) and the curvature ratio. (R/D). This regression analysis was carried out for all related parameters. By selecting a trendline to form a graph of the pressure drop coefficient correction factor equation with a temporary correction factor (ω_0), final correction factor (ω) and pressure drop coefficient ($\delta_a + \delta_b = C_{pd}$), with the subsequent pressure drop (Δ_p). If the curvature ratio (R/D) is 2, the equation is formed. $\omega_0 = 1.4092 n^{0.1867}$, $\omega = 1.3784 n^{0.2077}$, with $C_{pd-e} = 0.5342 n^{-0.409}$ and $C_{pd-pm} = 0.7326 n^{-0.208}$.

The physical model results of pressure drop with curvature ratio (R/D) 2 have a significant value compared to other R/D because the flow changes occur more suddenly compared to other smaller curvature ratios. Apart from that, the exponential equation has a positive power value because the curve formed by empirical data is lower than the physical model data, so it forms a rank equation

with a positive power. Meanwhile, Figure 3 with a curvature ratio (R/D) of 3, is relatively gentler because the turning radius is longer. The correction coefficient and pressure drop coefficient values formed are relatively smaller and the exponential equation has a negative value because the pressure drop data in the physical model is lower than the empirical simulation data.

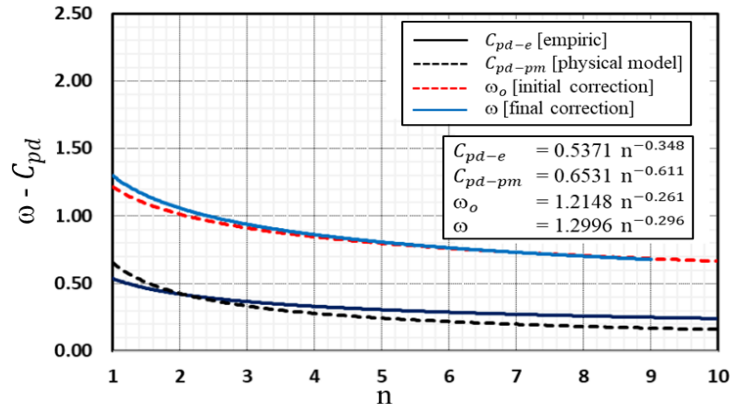


Fig. 3. Correction factor and pressure drop coefficient with the number of slice modifications (n) at R/D 3

While the curvature ratio (R/D) of 4 is also relatively gentler because the turning radius is longer. The values of the correction factor and pressure drop coefficient formed are relatively smaller. The resulting exponential equation is negative because the pressure drop data based on physical model data is lower than the empirical simulation data. In this condition, the equation is formed $\omega_o = 1.2757 n^{-0.322}$, $\omega = 1.4095 n^{-0.357}$, with $C_{pd-e} = 0.5406 n^{-0.292}$ and $C_{pd-pm} = 0.6901 n^{-0.615}$. Based on the equation that has been obtained, then validate the empirical equation with physical model data to determine the accuracy of the results of developing the equation with physical model data.

Validation of the empirical equation results is carried out by simulating the physical model data obtained for all equations. In this way, the empirical development results (corrected) are then compared with the physical model data obtained. The development of empirical equations uses simulated empirical equation data, which is corrected by calculating the pressure drop (Δ_p) = C_{pd} ($U^2/2g$), with $C_{pd} = \omega (\delta_a + \delta_b)$ against all conditions of curvature ratio (R/D) and slice modification (n). Next, perform statistical tests on the results of developing empirical equations to determine the accuracy of the model regarding the results of developing empirical equations that have been carried out, such as testing the initial empirical equation data that has been carried out previously.

Based on the results of the above process by displaying all slice modification models (n) and curvature ratios (R/D) according to the formation and combination of accompanying parameters, the overall model accuracy test results that have been obtained essentially meet the requirements for model suitability, including the correction factor (ω) and pressure drop coefficient (C_{pd}) and pressure drop (Δ_p). This is achieved by filtering the physical model data against the data trends that are formed and reducing the existing data deviation zones. Apart from that, this development model is an empirical model to obtain results that are close to physical model data as validation data so that the desired accuracy can be achieved.

The following is a complete description of the development of the model from empirical equations as shown below. The description of the pressure drop coefficient (C_{pd}) values for various variations of slice modification bends (n) and various curvature ratios (R/D), which are completely shown in the following table.

Table 2
 Pressure drop coefficient with variations in slice modification bends (n) and curvature ratio (R/D)

Curvature ratio	Parameter	Empirical model	(C_{pd}) , results of empirical model development					Notes
			n1	n2	n3	n4	n5	
R/D = 2	Δ_p	$1.3784 n^{0.2077} [\delta_a + \delta_b]$ [$U^2/2g$]	0.7363	0.6404	0.5902	0.5570	0.5326	
	C_{pd}	$1.3784 n^{0.2077} [\delta_a + \delta_b]$	0.7363	0.6404	0.5902	0.5570	0.5326	
R/D = 3	Δ_p	$1.2996 n^{-0.2296} [\delta_a + \delta_b]$ [$U^2/2g$]	0.6980	0.4467	0.2859	0.2859	0.2476	
	C_{pd}	$1.2996 n^{-0.2296} [\delta_a + \delta_b]$	0.6980	0.4467	0.2859	0.2859	0.2476	
R/D = 4	Δ_p	$1.4095 n^{-0.357} [\delta_a + \delta_b]$ [$U^2/2g$]	0.7620	0.4859	0.3099	0.3099	0.2681	
	C_{pd}	$1.4095 n^{-0.357} [\delta_a + \delta_b]$	0.7620	0.4859	0.3099	0.3099	0.2681	

Source: Analysis result

Based on Table 2. The value of the pressure drop coefficient (C_{pd}) for various variations of slice modification bends (n) and the curvature ratio (R/D) from the results of developing an empirical model regarding pressure drop (Δ_p), is completely shown in the following table.

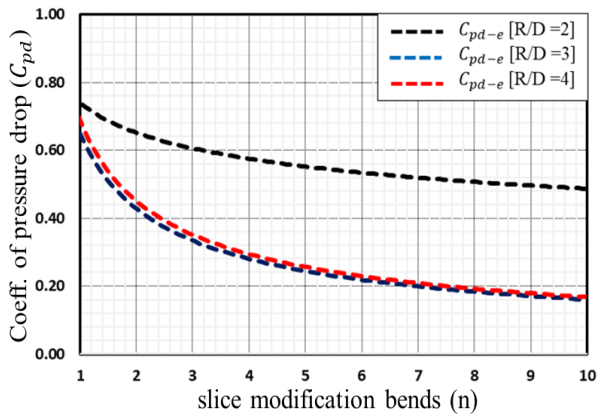


Fig. 4. Empirical pressure drop coefficient (C_{pd}) for varying curvature ratios (R/D 2, 3 and 4)

To simplify the implementation in calculating the pressure drop in each bend, the next step is to develop the empirical model practically and effectively by making the curvature ratio (R/D) flexible and determining the bend model (n) discretely, which will make it easier to implement and use this empirical model. in the analysis, as described in Table 3 and Figure 5 below.

Table 3
 The correction factor (ϖ) is based on the slice modification bend (n) and various curvature ratios R/D

Curvature ratio (R/D)	ϖ based on slice modification bends (n)									
	1	2	3	4	5	6	7	8	9	10
2	1.3784	1.5918	1.7317	1.8383	1.9255	1.9998	2.0649	2.1230	2.1756	2.2237
3	1.2996	1.0585	0.9388	0.8622	0.8971	0.7647	0.7306	0.7023	0.6782	0.6574
4	1.4095	1.1005	0.9522	0.8593	0.7935	0.7435	0.7037	0.6709	0.6433	0.6195

Source: Analysis result

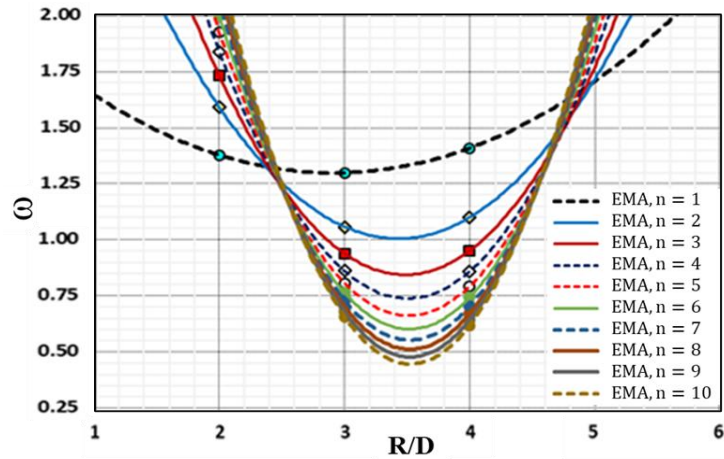
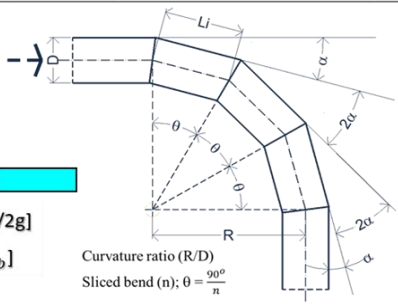


Fig. 5. Relationship between correction factor (ϖ) and curvature ratio (R/D)

Based on Figure 5, the equation formed is:

$\varpi = 0.0944 (R/D)^2 - 0.5506 (R/D) + 2.1021; n = 1$	$\varpi = 0.6070 (R/D)^2 - 4.2701 (R/D) + 8.1121; n = 6$
$\varpi = 0.2876 (R/D)^2 - 1.9715 (R/D) + 4.3843; n = 2$	$\varpi = 0.6537 (R/D)^2 - 4.6030 (R/D) + 8.6559; n = 7$
$\varpi = 0.4031 (R/D)^2 - 2.8086 (R/D) + 5.7363; n = 3$	$\varpi = 0.6947 (R/D)^2 - 4.8942 (R/D) + 9.1326; n = 8$
$\varpi = 0.4866 (R/D)^2 - 3.4092 (R/D) + 6.7103; n = 4$	$\varpi = 0.7312 (R/D)^2 - 5.1535 (R/D) + 9.5577; n = 9$
$\varpi = 0.5524 (R/D)^2 - 3.8806 (R/D) + 7.4770; n = 5$	$\varpi = 0.7642 (R/D)^2 - 5.3875 (R/D) + 9.9418; n = 10$

To simplify and abbreviate this empirical equation, this factored empirical equation is hereinafter referred to as the EMA equation. This writing designation is for simplicity and as a tribute to the research team involved. To determine effectiveness and optimality based on the equation in Figure 5 above, then tabulated as described in Figure 6 below this.

Curvature ratio (R/D)	ϖ										Geometry of 90-degree bend modification										
	n=1	n=2	n=3	n=4	n=5	n=6	n=7	n=8	n=9	n=10											
0.50	1.850	3.465	4.433	5.127	5.675	6.129	6.518	6.859	7.164	7.439											
1.00	1.646	2.680	3.331	3.788	4.149	4.449	4.707	4.933	5.135	5.319											
1.50	1.489	2.029	2.430	2.691	2.899	3.073	3.222	3.354	3.473	3.580											
2.00	1.379	1.512	1.732	1.838	1.925	2.000	2.065	2.123	2.176	2.224											
2.50	1.316	1.128	1.234	1.229	1.228	1.231	1.234	1.239	1.244	1.249											
3.00	1.300	0.878	0.938	0.862	0.807	0.765	0.730	0.702	0.678	0.657											
3.50	1.331	0.762	0.844	0.739	0.662	0.602	0.553	0.513	0.478	0.447	OPTIMUM										
4.00	1.410	0.780	0.951	0.859	0.793	0.744	0.703	0.671	0.643	0.619											
4.50	1.536	0.931	1.260	1.223	1.200	1.188	1.180	1.176	1.174	1.173											
5.00	1.709	1.217	1.771	1.829	1.884	1.937	1.983	2.029	2.070	2.109											
5.50	1.929	1.636	2.483	2.679	2.844	2.988	3.114	3.229	3.332	3.428											
6.00	2.197	2.189	3.396	3.773	4.080	4.344	4.571	4.777	4.960	5.128											
Curvature ratio (R/D)	δ_a/f										δ_b										
	n=1	n=2	n=3	n=4	n=5	n=6	n=7	n=8	n=9	n=10	n=1	n=2	n=3	n=4	n=5	n=6	n=7	n=8	n=9	n=10	
	$\delta_a/f = [(n \cdot L_i)/D]$										$\delta_b = [1 - \cos^2 \alpha \cdot \cos^{(n-1)} 2\alpha]$										
0.50	0.707	0.765	0.776	0.780	0.782	0.653	0.560	0.490	0.436	0.392	0.500	0.396	0.300	0.241	0.202	0.173	0.152	0.135	0.122	0.111	
1.00	1.414	1.531	1.553	1.561	1.564	1.305	1.120	0.980	0.872	0.785	0.500	0.396	0.300	0.241	0.202	0.173	0.152	0.135	0.122	0.111	
1.50	2.121	2.296	2.329	2.341	2.347	1.958	1.679	1.470	1.307	1.177	0.500	0.396	0.300	0.241	0.202	0.173	0.152	0.135	0.122	0.111	
2.00	2.828	3.061	3.106	3.121	3.129	2.611	2.239	1.960	1.743	1.569	0.500	0.396	0.300	0.241	0.202	0.173	0.152	0.135	0.122	0.111	
2.50	3.536	3.827	3.882	3.902	3.911	3.263	2.799	2.450	2.179	1.961	0.500	0.396	0.300	0.241	0.202	0.173	0.152	0.135	0.122	0.111	
3.00	4.243	4.592	4.659	4.682	4.693	3.916	3.359	2.941	2.615	2.354	0.500	0.396	0.300	0.241	0.202	0.173	0.152	0.135	0.122	0.111	
3.50	4.950	5.358	5.435	5.463	5.475	4.568	3.919	3.431	3.050	2.746	0.500	0.396	0.300	0.241	0.202	0.173	0.152	0.135	0.122	0.111	
4.00	5.657	6.123	6.212	6.243	6.257	5.221	4.479	3.921	3.486	3.138	0.500	0.396	0.300	0.241	0.202	0.173	0.152	0.135	0.122	0.111	
4.50	6.364	6.888	6.988	7.023	7.040	5.874	5.038	4.411	3.922	3.531	0.500	0.396	0.300	0.241	0.202	0.173	0.152	0.135	0.122	0.111	
5.00	7.071	7.654	7.765	7.804	7.822	6.526	5.598	4.901	4.358	3.923	0.500	0.396	0.300	0.241	0.202	0.173	0.152	0.135	0.122	0.111	
5.50	7.778	8.419	8.541	8.584	8.604	7.179	6.158	5.391	4.794	4.315	0.500	0.396	0.300	0.241	0.202	0.173	0.152	0.135	0.122	0.111	
6.00	8.485	9.184	9.317	9.364	9.386	7.832	6.718	5.881	5.229	4.708	0.500	0.396	0.300	0.241	0.202	0.173	0.152	0.135	0.122	0.111	

Notes: The friction coefficient (f) is based on the Moody diagram or trial and error on the flow and type of pipe
 Source: Analysis result

Fig. 6. The pressure drop coefficient in a modified 90-degree slice bend is based on the EMA equation

Based on the table above, the value of the pressure drop coefficient (C_{pd}), it is necessary to know the friction coefficient (f) and choose the curvature ratio (R/D) and the number of slices modification bend (n). By selecting R/D, you select the radius of the bend as well as the diameter of the pipe to be used. By using a Moody diagram or trial and error, the friction coefficient (f) can be obtained according to the fluid flowing, the diameter and the type of pipe used. If the friction coefficient has been determined, the pressure drop coefficient value is corrected as (C_{pd}) = $\varpi (\delta_a + \delta_b)$.

To find alternative parameters that provide optimal results in research modelling, sensitivity analysis is needed. Sensitivity analysis in determining research modelling parameters has an optimization function in determining risks and cost benefits in the business and industrial fields. In the field of management and operations, it has the function of maximizing efficiency, while in the field of research and model development, the function is to determine parameter limits to obtain the best model to provide recommendations for the performance to be achieved.

The sensitivity analysis process in this research is to enter new parameters into the equation. The new parameter is the correction factor for the pressure drop coefficient (ϖ) both caused by pipe wall friction (δ_a) and caused by changes in flow direction (δ_b) in physical model data with empirical data. The pressure drop coefficient correction factor applies to all curvature ratios and slice modification bend models. In this analysis using physical model data, in addition to knowing the capabilities of the new parameters that appear, it is also possible to add treatment to variations in flow rate for pressure drop (Δ_p) and add variations to the slice modification bend model (n) to form a more perfect graph.

The service capabilities demonstrated by the slice modified of the bend model in this research are the flexibility of the model and the equation for the efficiency of pressure drop by the bend model when it is in operation. The bend performance in this study is shown by the pressure drop coefficient ratio value based on the comparison between the pressure drop coefficient compared to the slice-modified bend arm. Based on the results of the pressure drop simulation and the graph of the relationship between pressure drop (Δ_p) and pressure height due to flow ($U^2/2g$), pressure drop ratio

(Δ_p/Li) , head pressure ratio due to flow velocity $[(U^2/2g)/D]$ and a graph of the relationship between pressure drop (Δ_p) and flow rate (Q).

From these graphs at a curvature ratio (R/D) of 2, the modified bend model whose flow performance is unbalanced is modified bend (n) = 2, the results of the physical model with empirical data are significantly different, most likely due to back pressure that occurs due to downstream of the bend, the physical model data has a much different trend compared to other physical model data. Meanwhile, at a curvature ratio (R/D) of 3, the level of performance displayed is somewhat different in the bend model (n) = 5, the results of the physical model with the development of the empirical model have a trend that is slightly away from the physical model data. At a curvature ratio (R/D) of 4, the performance shown by the development of the empirical model as a whole is close to the same as the data from the physical model and the trends formed are also in line with the data from the physical model.

The basic nature or character of flow and the dynamics or behaviour of flow in a closed pipe have a close relationship and are interrelated. These related elements include speed, roughness, fluid viscosity and pipe diameter. Pipe flow Osborn Reynold [10,30], stated that flow in a pipe at a number $Re < 2000$, the flow disturbance can be resisted by the viscosity of the fluid, is called laminar flow, flow that has a number $Re > 4000$ is called turbulent flow. Meanwhile, flows with Reynolds numbers include those called transition flows.

According to the law of frictional resistance, the logarithmic graph of the ratio between pressure drop (Δ_p) and flow velocity (U), from a linear graph is formed with the value $\tan \alpha = 1$ or $\log U = \log \Delta_p$ atau $\Delta_p = C.U$, in this condition the flow fluctuation What happens is still able to be resisted by the viscosity of the fluid and is called laminar flow. It is said to be a transition zone if the value of $\tan \alpha = 1.75 - 2.00$, also known as an unstable (transition) zone. If $\tan \alpha$ is greater than 2.00 or the Reynolds number (Re) > 4000 then the zone is a zone of irregular turbulence or turbulence occurs which is called turbulent flow.

The results of the analysis of flow characteristics based on physical model data at a curvature ratio (R/D) = 2, Re value > 4000 , show that the overall flow is turbulent. Likewise, the linear equation graph uses the original data distribution, the value of $\tan \alpha > 2$ so that the flow is also turbulent. Meanwhile, in the flow before entering the bend and after passing through the bend in all the slice modification bends (n1 – n5) the flow is transitional except after n5 there is laminar flow because the value of $\tan \alpha < 1$. This shows that the flow through the slice-modified curved pipe tends to experience turbulence or irregular flow, resulting in turbulence.

Likewise, what happens at the curvature ratio (R/D) = 3, Re value > 4000 , the flow is turbulent. In the linear equation graph of the original data distribution, the value $\tan \alpha > 2$ also represents turbulent flow. However, before and after the turn there is a transitional and turbulent flow throughout. Meanwhile, the flow characteristics that occur in the modified slice bend model with a curvature ratio (R/D) = 4 are turbulent flows because Reynolds number (Re) > 4000 . Based on the physical model data distribution, it shows that there is a transition flow because of the ratio of $\log U$ and $\log \Delta_p < 2$. Meanwhile, the characteristics and flow behavior that occurs in bends based on Ansys simulations using a modified 90-degree slice bend model at n1 to n3 at a bend curvature ratio (R/D) of 2 and a flow rate of 0.50 l/s are described as explained below.

Based on the visual simulation of flow in a modified slice bend model (n) 1 with a curvature ratio (R/D) 2 as in Figure 7, the flow that occurs when passing through a bend occurs turbulence and vortexes appear on the sides of the corners in the bend and appear as shown in section 2 to section 5.

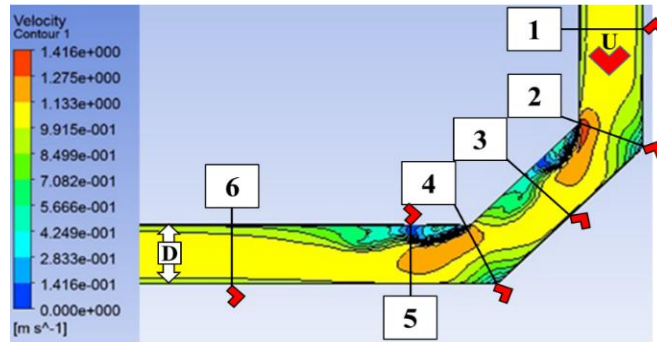


Fig. 7. Flow behaviour in slice modification bends (n) 1 with curvature ratio (R/D) 2

Meanwhile, transition flow occurs before entering the curve as depicted in section 1 and some distance after passing through the bends as depicted in section 6.

Likewise, in modified slice bends with the number of slices (n) 2 with a curvature ratio (R/D) 2 as in Figure 8, the flow that occurs when passing through a bend occurs turbulence and vortices appear to occur on all sides of the corner in the bend, but the vortex starts to get smaller because the number of cuts increases or the angle of change of direction decreases and appears as shown in cut 2 to cut 5. Meanwhile, the transition flow occurs before entering the bend as depicted in section 1 and some distance after passing the curve as depicted in section 6.

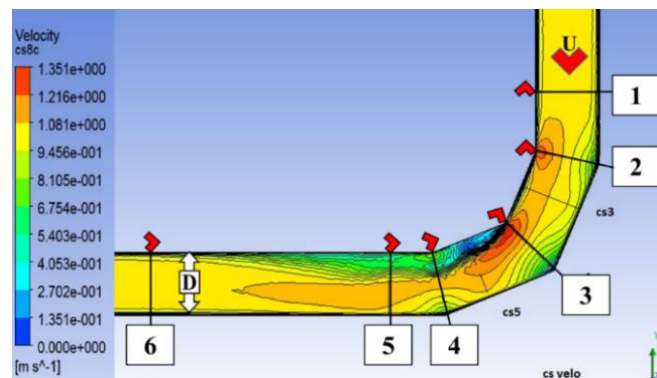


Fig. 8. Flow behaviour in slice modification bends (n) 2 with curvature ratio (R/D) 2

Meanwhile, also in modified curves, the slices have many slices (n) of 3 with a curvature ratio (R/D) of 2 as in Figure 9, the flow that occurs when passing through a bend still has turbulence and appears the vortex on all sides of the corners in the bend but the vortex has weakened because the number of slices is increasing or the angle of change of direction is smaller than the previous bend and appears as shown in section 2 to piece 5. Meanwhile, the transition flow occurs before entering the bend as depicted in Section 1 and some distance after passing the curve as depicted in Section 6.

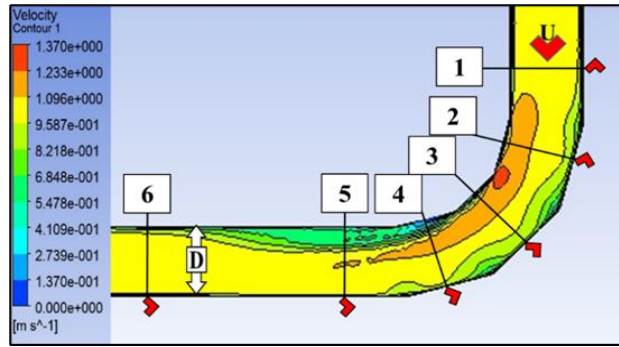


Fig. 9. Flow behaviour in slice modification bends (n) 3 with curvature ratio (R/D) 2

By following the hypothesis of this research, the modified 90-degree angle bend with slices means that the more the number of slices that form it, the smoother the shape of the bend will be, resembling a curved bend and the resulting pressure drop coefficient will be smaller. This has been proven by the performance and characteristics described above. Below, an EMA equation model is simulated to prove the hypothesis about slice modification bends with an unlimited number of slices (n) which are identical to curved bends. This is proven by the empirical models of Triatmodjo [28] and Nakayama [23] with curvature ratios (R/D) 2 and 4 which are implemented at a bend angle of 90-degree as in Table 4 below.

Table 4

Simulation of the EMA empirical model with other empirical models

slice bends (n)	90-degree bend with R/D = 2		slice bends (n)	90-degree bend with R/D = 4		Notes
	C_{pd}	Triatmodjo [28]	C_{pd}	Triatmodjo [28]	Nakayama [23]	
	EMA = $n^{-0.208}$		EMA = $n^{-0.615}$			
1	0.7326		1	0.6901		
5	0.5242		5	0.2565		Triatmodjo [28]
10	0.4538		10	0.1675	0.1700	curved bend 90-degree
30	0.3611		30	0.0852		
50	0.3247		50	0.0622		
100	0.2811		100	0.0406		
200	0.2434		200	0.0265		
300	0.2237		300	0.0207		Nakayama [23]
400	0.2107		400	0.0173		curved bend 90-degree
600	0.1936	0.1900	600	0.0135		
800	0.1824		800	0.0113		
1000	0.1741		1000	0.0099		
2000	0.1507		2000	0.0064		
3000	0.1386		3000	0.0050		
					0.1350	

Source: Analysis result

Based on Table 4, it can be concluded that the empirical equation obtained by simulating an infinite number of slice models (n), the pressure drop coefficient value obtained is identical to the curved bends of previous researchers. Although this situation is impossible to implement because of the level of difficulty if the number of n is infinite, it is recommended with a value of n between 1 and 5 considering efficiency in the field. According to Table 4 above, the pressure drop coefficient value of the EMA equation is close to the pressure drop coefficient value in curved bends like the

Triatmodjo [28] and Nakayama [23] empirical models. This shows that the resulting equation is very significant following the hypothesis and research objectives and complements previous research.

The final equation for pressure drop (Δ_p) of 90-degree bend with slice modification, $\Delta_p = C_{pd} (U^2/2g)$ and the pressure drop coefficient equation (C_{pd}) = $\omega(\delta_a + \delta_b)$, with values $\delta_a = f [(n \cdot Li)/D]$ and $\delta_b = (1 - \cos^2 \alpha \cos^{(n-1)} 2\alpha)$, as well as $\omega = 1.3784 n^{0.2077}$ at $R/D = 2$, $\omega = 1.2996 n^{-0.296}$ at $R/D = 3$ and $\omega = 1.4095 n^{-0.357}$ at $R/D = 4$. The results of the model accuracy test from this equation are $NSE = -0.632$ to $+0.994$, $MAE = +0.021$ to $+1.699$ and $RMSE = +0.031$ to $+1.817$.

4. Conclusion

Flow behaviour in modified bend with variations of curvature ratio (R/D) and slice modification model (n) obtained by Reynolds number values (Re) = $26.13 - 67.44 \times 106$ ($R/D=2$), $Re = 29.33 - 64.87 \times 106$ ($R/D=3$) and $Re = 31.01 - 62.36 \times 106$ ($R/D=4$) so the occurs of flow varies from laminar to turbulent. Based on the Ansys simulation at the $R/D = 2$ and with n of 1, 2 and 3 forming a vortex on the inner side of the impeller, the occurs of vortex due to a sudden change in direction, this shows that with the n of 1, the angle of change in direction sharper and the vortex more extreme, whereas the greater of n , the angle of change in direction smaller, the vortex smaller and even disappears. The correction factor (ϖ) for the obstacle coefficient obtained from the previous research equation is $\varpi = 1.3784 n^{0.2077}$ for R/D of 2, $\varpi = 1.2996 n^{-0.296}$ for R/D of 3, dan $\varpi = 1.4095 n^{-0.357}$ for R/D of 4. NSE model accuracy test results = -0.632 up to $+0.994$, $MAE = +0.021$ up to $+1.699$ and $RMSE = +0.031$ up to $+1.817$. The influence that occurs due to flow behaviour with variations in R/D and n on the pressure drop is the smaller, the smaller R/D and the smaller n so, the flow changes become more sudden and form a vortex at the inner corner of the bend. The vortex that appears is a series of flow turbulence occurring at n and based on Ansys simulations, turbulence symptoms form when the flow approaches the bend. Turbulence flow is the cause of the large pressure drop.

Following Eq. (1) and Table 1, to determine the magnitude of the friction factor (f), it is influenced by the viscosity of the fluid, the value of which depends on the type and temperature of the fluid as well as the roughness of the channel walls, according to Moody's principle. The flow velocity (U) in the pipe due to the water level (H) in the reservoir or other is $U^2=2gH$, with pressure drop (Δ_p) = $C_{pd} [U^2/2g]$ (see Table 2). Fluid flowing in a bend that originates from a straight pipe will be forced according to the bend it is passing through. As a result, the occurs of the straight pressure, the outer pipe bend side experiences scouring due to maximum pressure. Meanwhile, on the inside of the bend, vortices and turbulence will occur due to the flow velocity being blocked or colliding with the flow on the outside of the bend. This turbulence phenomenon then triggers deposition on the inside of the bend. In curved pipe bends, this condition occurs more smoothly, whereas in slice bends the modification occurs sporadically. This happens more sporadically when the bends use a smaller number of slices (n).

Acknowledgment

This work is supported by the University of Muhammadiyah Malang and we would like to thank all leaders and staff for all their support.

References

- [1] Abbaszadeh, Hamidreza, Reza Norouzi, Veli Süme, Rasoul Daneshfaraz, and Reza Tarinejad. "Discharge coefficient of combined rectangular-triangular weirs using soft computing models." *Journal of Hydraulic Structures* 9, no. 1 (2023): 98-110.

- [2] Abduh, Moh. "Measurement of discharge in open channels: A case study of laboratory discharge calibration model." In *AIP Conference Proceedings*, vol. 2453, no. 1. AIP Publishing, 2022. <https://doi.org/10.1063/5.0094277>
- [3] Abduh, Moh, Suhardjono Suhardjono, Sumiadi Sumiadi, and Very Dermawan. "The coefficient of head loss at the pipe bend 90 with the sliced bend." *Journal of Water and Land Development* 46 (2020). <https://doi.org/10.24425/jwld.2020.134083>
- [4] Abduh, Moh, and Very Dermawan. "Simplified Equations and Ansys Simulation of Head Loss on Nonlinear (Sliced) Bend for Piping Network." In *Journal of Physics: Conference Series*, vol. 1477, no. 5, p. 052002. IOP Publishing, 2020. <https://doi.org/10.1088/1742-6596/1477/5/052002>
- [5] Abduh, Moh, and Very Dermawan. "The behaviour of fluid flow in a 90-degree (sliced) nonlinear bend." In *IOP Conference Series: Earth and Environmental Science*, vol. 437, no. 1, p. 012001. IOP Publishing, 2020. <https://doi.org/10.1088/1755-1315/437/1/012001>
- [6] Adjei, R., and Ali Mohsin. "Simulation-driven design o optimization: A case study on a double 90 elbow bend." *International Journal of Modeling and Optimization* 4, no. 6 (2014): 426-432. v
- [7] Ayala, Manuel, and John M. Cimbala. "Numerical approach for prediction of turbulent flow resistance coefficient of 90 pipe bends." *Proceedings of the Institution of Mechanical Engineers, Part E: Journal of Process Mechanical Engineering* 235, no. 2 (2021): 351-360. <https://doi.org/10.1177/0954408920964008>
- [8] Barkley, Dwight. "Theoretical perspective on the route to turbulence in a pipe." *Journal of Fluid Mechanics* 803 (2016): P1. <https://doi.org/10.1017/jfm.2016.465>
- [9] Chowdhury, Rana Roy, Md Mahbubul Alam, and AKM Sadrul Islam. "Numerical modeling of turbulent flow through bend pipes." *environment* 6, no. 7 (2016).
- [10] Zuck, D. "Osborne reynolds, 1842-1912, and the flow of fluids through tubes." *British journal of anaesthesia* 43, no. 12 (1971): 1175-1182. <https://doi.org/10.1093/bja/43.12.1175>
- [11] Drikakis, Dimitris, Ioannis William Kokkinakis, Daryl Fung, and S. Michael Spottswood. "Generalizability of transformer-based deep learning for multidimensional turbulent flow data." *Physics of Fluids* 36, no. 2 (2024). <https://doi.org/10.1063/5.0189366>
- [12] Dutta, Prasun, and Nityananda Nandi. "Effect of Reynolds number and curvature ratio on single phase turbulent flow in pipe bends." *Mechanics and Mechanical Engineering* 19, no. 1 (2015): 5-16.
- [13] Dutta, P., S. K. Saha, and N. Nandi. "Numerical study of curvature effect on turbulent flow in 90 pipe bend." *Dep. of Aerospace Eng. and Applied Mechanics, ICTACEM-2014/028* (2014).
- [14] Eckert, Michael. "Pipe flow: a gateway to turbulence." *Archive for History of Exact Sciences* 75, no. 3 (2021): 249-282. <https://doi.org/10.1007/s00407-020-00263-y>
- [15] Gajbhiye, Bhavesh D., Harshawardhan A. Kulkarni, Shashank S. Tiwari, and Channamallikarjun S. Mathpati. "Teaching turbulent flow through pipe fittings using computational fluid dynamics approach." *Engineering Reports* 2, no. 1 (2020): e12093. <https://doi.org/10.1002/eng2.12093>
- [16] Hassanzadeh, Yousef, and Hamidreza Abbaszadeh. "Investigating discharge coefficient of slide gate-sill combination using expert soft computing models." *Journal of Hydraulic Structures* 9, no. 1 (2023): 63-80.
- [17] Hu, Dong-fang, Zheng-liang Huang, Jing-yuan Sun, Jing-dai Wang, Zu-wei Liao, Bin-bo Jiang, Jian Yang, and Yong-rong Yang. "Numerical simulation of gas-liquid flow through a 90° duct bend with a gradual contraction pipe." *Journal of Zhejiang University-SCIENCE A* 18, no. 3 (2017): 212-224. <https://doi.org/10.1631/jzus.A1600016>
- [18] Wan, Kai, and Ping Wang. "CFD numerical simulation analysis of small and medium caliber 90 circular bend." In *Conference of the 2nd International Conference on Computer Science and Electronics Engineering (ICCSEE 2013)*, pp. 105-107. Atlantis Press, 2013. <https://doi.org/10.2991/iccsee.2013.27>
- [19] Kim, Jongtae, Mohan Yadav, and Seungjin Kim. "Characteristics of secondary flow induced by 90-degree elbow in turbulent pipe flow." *Engineering Applications of Computational Fluid Mechanics* 8, no. 2 (2014): 229-239. <https://doi.org/10.1080/19942060.2014.11015509>
- [20] Kumar, Shivam, Mukund Kumar, Samiran Samanta, Manoj Ukamanal, Asisha Ranjan Pradhan, and Shashi Bhushan Prasad. "Simulations of water flow in a horizontal and 900 pipe bend." *Materials Today: Proceedings* 56 (2022): 889-895. <https://doi.org/10.1016/j.matpr.2022.02.528>
- [21] Mathias, Simon A. "Flow in Pipes and Normal Flow in Open Channels." In *Hydraulics, Hydrology and Environmental Engineering*, pp. 37-60. Cham: Springer International Publishing, 2024. https://doi.org/10.1007/978-3-031-41973-7_2
- [22] Najjari, Mohammad Reza, Christopher Cox, and Michael W. Plesniak. "Formation and interaction of multiple secondary flow vortical structures in a curved pipe: Transient and oscillatory flows." *Journal of Fluid Mechanics* 876 (2019): 481-526. <https://doi.org/10.1017/jfm.2019.510>
- [23] Nakayama, Yasuki. *Introduction to fluid mechanics*. Butterworth-Heinemann, 2018. <https://doi.org/10.1016/B978-0-08-102437-9.00001-2>

- [24] Pradhan, Asisha Ranjan, Satish Kumar, Shalendra Kumar, Harmanpreet Singh, Kaushal Kumar, and Gurmeet Singh. "Prediction of head loss for fly ash-water slurry flow through 90° bend pipe using computational fluid dynamics." *Materials Today: Proceedings* 56 (2022): 710-716. <https://doi.org/10.1016/j.matpr.2022.01.197>
- [25] Rathore, Manish Kumar, Dilbag Singh Mondloe, and Satish Upadhyay. "Computational investigation of fluid flow 90 bend pipe using finite volume approach." *International Research Journal of Engineering and Technology (IRJET)* 4, no. 06 (2017).
- [26] Sumiadi, Sumiadi, and Moh Abduh. "Mean flow characteristics in a flat and eroded bed curved channel." *Journal of Water and Land Development* (2022). <https://doi.org/10.24425/jwld.2022.140794>
- [27] Taira, Kunihiko, and Aditya G. Nair. "Network-based analysis of fluid flows: Progress and outlook." *Progress in Aerospace Sciences* 131 (2022): 100823. <https://doi.org/10.1016/j.paerosci.2022.100823>
- [28] Triatmodjo, Bambang. "Hidrolika II." *Beta Offset, Yogyakarta* (1993).
- [29] Vollestad, P., L. Angheluta, and A. Jensen. "Experimental study of secondary flows above rough and flat interfaces in horizontal gas-liquid pipe flow." *International Journal of Multiphase Flow* 125 (2020): 103235. <https://doi.org/10.1016/j.ijmultiphaseflow.2020.103235>
- [30] Wu, Xiaohua, Parviz Moin, Ronald J. Adrian, and Jon R. Baltzer. "Osborne Reynolds pipe flow: Direct simulation from laminar through gradual transition to fully developed turbulence." *Proceedings of the National Academy of Sciences* 112, no. 26 (2015): 7920-7924. <https://doi.org/10.1073/pnas.1509451112>
- [31] Zhang, Jianyi, Dongrui Wang, Weiwei Wang, and Zuchao Zhu. "Numerical investigation and optimization of the flow characteristics of bend pipe with different bending angles." *Processes* 10, no. 8 (2022): 1510. <https://doi.org/10.3390/pr10081510>
- [32] Zhang, Ke-dong, Wen-hua Wang, Hao Yang, Lin-lin Wang, Ya-zhen Du, and Yi Huang. "Mechanism analysis of secondary flow and mechanical energy loss in toroidal flow field." *Physics of Fluids* 36, no. 2 (2024). <https://doi.org/10.1063/5.0180572>
- [33] Zhang, Songsong, Baohuan Su, Jianmin Liu, Xuemin Liu, Guoli Qi, and Yajun Ge. "Analysis of flow characteristics and flow measurement accuracy of elbow with different diameters." In *IOP Conference Series: Earth and Environmental Science*, vol. 113, no. 1, p. 012231. IOP Publishing, 2018. <https://doi.org/10.1088/1755-1315/113/1/012231>
- [34] Zheng, Weixiong, Dongjie Wang, Fuyan Lyu, Yang Shen, Yue Pan, and Miao Wu. "Influence of elasticity of high-concentration paste on unsteady flow in pipeline transportation." *Physics of Fluids* 36, no. 1 (2024). <https://doi.org/10.1063/5.0176824>